

Numerical field evaluation of healthcare workers when bending towards high-field MRI magnets

H. Wang¹, A. Trakic¹, F. Liu¹, and S. Crozier¹

¹The School of Information Technology and Electrical Engineering, The University of Queensland, Brisbane, Queensland, Australia

Synopsis: In MRI, healthcare workers may be exposed to strong static and dynamic magnetic fields outside of the imager. Presented are numerical evaluations of electric fields/currents in anatomically-equivalent male and female human models (healthcare workers) as they lean towards the bores of three superconducting magnet models (1.5T, 4T and 7T) and x, y and z- gradient coils. The combined effect of the 1.5T superconducting magnet and the three gradient coils on the body models is compared with the contributions of the magnet and gradient coils separately. The simulation results indicate that it is possible to induce field quantities above regulatory guidelines, especially when the MRI operator is bending close towards the main magnet and all three gradient coils are switched simultaneously.

Method: Three realistic symmetric superconducting magnets (1.5T, 4T and 7T unshielded) and actively shielded, whole body, symmetric x, y and z-axis gradient coils were considered in this study. Tissue-equivalent whole-body male and female voxel phantoms (*Norman* and *Naomi*) were employed to accurately model the exposure of occupational workers to fields produced by the main magnet and gradient coils. The quasi-static finite-difference method was employed to compute the induced electric fields. For further details on the magnets, gradients, body model and the computational method, the reader is referred to (1). For the case of a body model that is leaning towards a main magnet, the assignment of velocities to model voxels undergoing a rotating motion is detailed. Each voxel in the upper half of the body model is physically rotated forward at an angle ϕ , relative to the bending pivot, as illustrated in Fig.1. Here, the bending pivot is treated as a line that is parallel to the x-axis and is located at the frontal body side/surface between the upper and lower half of the body model. The lower half of the voxel model remains stationary in this case. A back projection method is then engaged to match each voxel of the projected body to the original standing model.

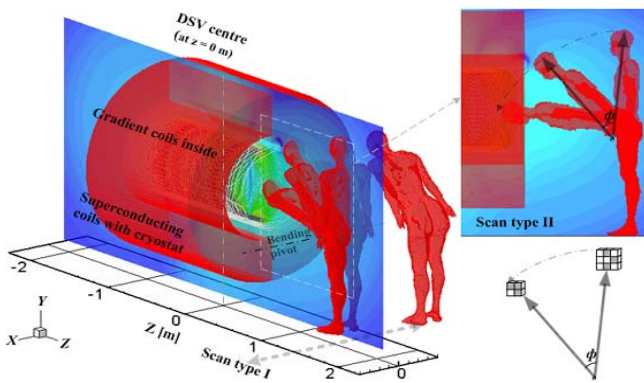


Fig.1 - Sketch of the male body model in front of the imager entrance. Illustrated are TYPE I and TYPE II region scan set-ups

Following model worker exposure scenarios were considered:

- i) Main 1.5T, 4T and 7T superconducting magnets (no pulsed gradients)
- ii) Combination of all three gradient coils (without static field gradients)
- iii) 1.5T magnet (with cryostat) and all three gradient coils

as the body models undergo a bending motion towards the bore entrance of the designated system. In evaluations ii) and iii), each gradient coil is assumed to produce a 40 mT/m gradient field within the imaging volume. In iii), the exposure to static and dynamic fields is modelled separately at first, after which the induced electric field components are added appropriately to obtain the combined effect of exposure. The minimum distance between the model surface and the imager end (including cryostat) was assumed to be 10 mm.

Results and discussion:

The average and 1%-thresholded values of **E**, **J** and 1 cm^2 -averaged **J** in selected tissues of Norman for all designated exposure cases

Case	Tissue	1.5T		4T		7T		Gradients		Combination	
		Avg	1%	Avg	1%	Avg	1%	Avg	1%	Avg	1%
E	CSF	22.50	74.68	48.19	173.75	71.82	254.71	229.20	469.64	251.70	544.32
	Brain	56.83	164.17	128.62	382.10	188.88	560.15	486.00	899.71	542.83	1063.88
	Spine	23.31	52.26	39.79	100.64	62.21	146.35	118.80	568.21	142.11	620.47
	Heart	29.35	68.27	47.34	110.91	74.75	173.26	86.40	170.89	115.75	239.16
	Skin	10.58	51.13	18.78	109.43	29.66	159.18	74.00	436.78	84.58	487.91
J	CSF	45.00	233.02	96.39	542.11	143.64	794.71	458.00	1465.44	503.00	1698.46
	Brain	1.56	4.36	3.54	10.15	5.20	14.87	48.00	85.79	49.56	90.15
	Spine	0.40	0.89	0.68	1.72	1.07	2.50	3.60	16.42	4.00	17.31
	Heart	1.58	3.67	2.54	5.95	4.01	9.32	9.20	18.22	10.78	21.89
	Skin	0.00	0.01	0.00	0.02	0.01	0.03	0.00	0.09	0.00	0.10
$1 \text{ cm}^2 J_{\text{avg}}$	CSF	19.29	46.25	40.67	107.98	60.76	158.29	212.40	387.68	231.69	433.94
	Brain	4.81	37.72	11.02	87.71	16.19	128.58	80.80	306.57	85.61	344.29
	Spine	7.01	23.57	11.64	37.92	18.31	61.46	34.00	200.21	41.01	223.78
	Heart	2.89	10.45	4.66	16.97	7.36	26.72	13.60	43.56	16.49	54.00
	Skin	0.20	2.86	0.36	6.76	0.56	9.92	2.00	18.04	2.20	20.91

Conductivities of tissue - CSF: 2.00 Sm^{-1} ; Brain: 0.03 Sm^{-1} ; Spine: 0.02 Sm^{-1} ; Heart: 0.05 Sm^{-1} ; Skin: $2.00\text{e-}4 \text{ Sm}^{-1}$; Fat: 0.01 Sm^{-1} ; Muscle: 0.20 Sm^{-1} .

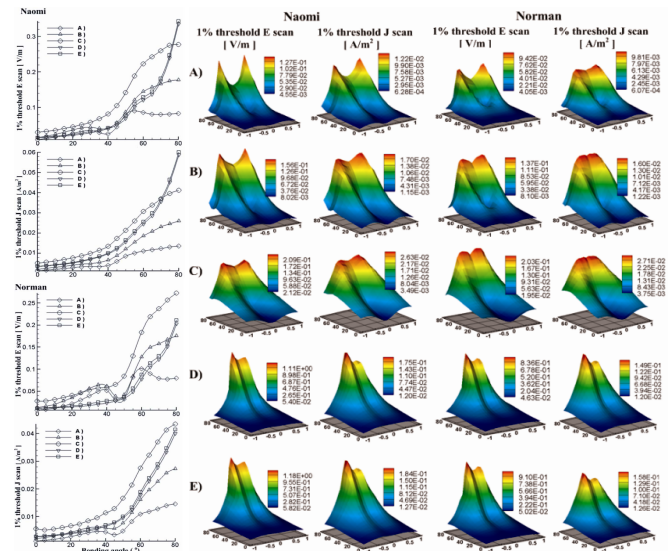


Fig.2 - Shown are records of induced electric field **E** and current density **J** for both the male and female body model. The subplots are in terms of exposures to: A) 1.5T, B) 4T C) 7T magnet, D) all three gradient coils and E) combination of 1.5T magnet and all three gradient coils: for type I (right) and type II (left) region scan.

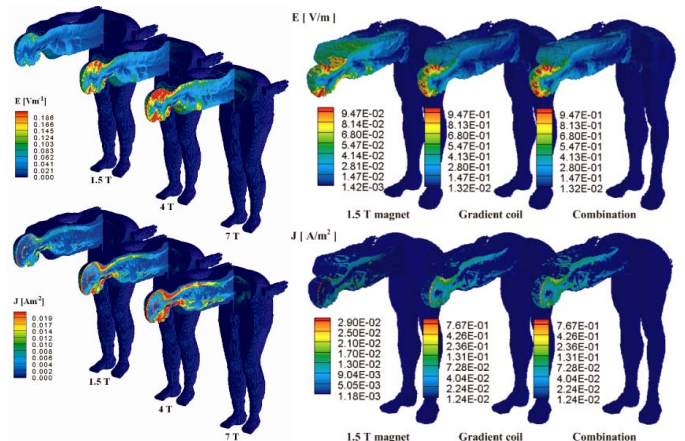


Fig.3 - Electric field and current density distributions at the maximum bend angle of 80° and radial position of $r = 0$: exposure of Naomi to the three main magnets (left) and exposure of Norman to the 1.5T magnet, three gradient coils as well as combination of the 1.5T magnet and the three gradient coils (right).

The induced E-fields increase for increasing bend angle. As the physiology and dielectric properties of each and every person is somewhat different, it is quite difficult to predict the exact mechanisms of induced fields and their effects on the physiology. It still remains unknown to what degree the low-frequency electromagnetic fields can be harmful to the humans in long-term exposures. Nevertheless, it is possible to gain useful information by evaluating the peak fields relative to different positions of the radiologist/technician around the imager and to use this to inform clinical practice.

Conclusion: The simulation results of healthcare worker exposure to gradient coils indicate that the induced field quantities can be of very similar magnitude as those induced in the patients during MRI imaging and therefore should not be ignored. More importantly it was observed that the field induction due to pulsed gradient coils dominates over the induction attributed to the body bending motion through non-uniform static magnetic fields.

Acknowledgements: Financial support for this project from the Australian Research Council and from the Health and Safety Executive (UK) managed by Microwave Consultants Limited (UK) are gratefully acknowledged. The authors thank the Oxford Magnet Technology for providing the 4T pattern.

References: [1] RR570 report, Health and Safety Executive, HSE Books, 2007.